PAPER

CrossMark
click for updates

Catalytic wet air oxidation of *m*-cresol over a surface-modified sewage sludge-derived carbonaceous catalyst†

Yang Yu,[ab] Huangzhao Wei,[a] Li Yu,[ab] Bin Gu,[ab] Xianru Li,[ab] Xin Rong,[a] Ying Zhao,[ab] Lili Chen[ab] and Chenglin Sun*[a]

Sewage sludge-derived carbonaceous materials (SW) treated with different kinds of acids were used as catalysts for catalytic wet air oxidation (CWAO) of *m*-cresol. The SW catalysts were characterized by XRF, XRD, FTIR, XPS and TPD-MS. The results showed that SW treated with HNO_3 (HNO_3-SW) exhibited the best catalytic activity. When the initial concentration of *m*-cresol was 5000 mg L^{-1}, the conversion of *m*-cresol reached 99.0% with HNO_3-SW after 90 min at 160 °C and 0.66 MPa oxygen. Continuous experiments were carried out for 8 d to investigate the durability and catalytic performance of HNO_3-SW in CWAO reaction. Some correlation was observed between the conversion of *m*-cresol and the content of carboxyl groups, indicating that the carboxyl group might play a key role in determining the catalytic activity of SW catalysts in CWAO reaction. Based on the intermediate products identified by GC-MS, HPLC-MS, IC and HRMS analyses, the oxidation pathways of *m*-cresol in CWAO were proposed.

1. Introduction

Over the past decade, the increase in number of wastewater treatments has produced a dramatic amount of sewage sludge.[1] The disposal of sewage sludge has been a serious environmental problem.[2] Common disposal methods of sewage sludge including ocean dumping, landfill disposal and application to farmland may cause secondary pollution to ocean, soil and ground water.[3] Therefore, many studies have focused on the recycling of sewage sludge. Sewage sludge pyrolysis is considered as an attractive technique and develops rapidly since it is effective in reducing the volume of sludge and producing bio-oil.[4,5] Sewage sludge-derived carbonaceous materials (SW) produced during the pyrolysis of sewage sludge were used as adsorbents for air pollution, organic pollutants and heavy metals in the past.[6,7] Nowadays, numerous research studies have been carried out to apply SW as a catalyst in wastewater treatment, such as catalytic wet air oxidation (CWAO),[1,8,9] catalytic ozone oxidation[10] and Fenton-like oxidation.[11,12] Stüber first reported the application of SW

in CWAO reaction.[8] Marques found the correlation between the surface area of SW and catalytic activity.[1] Yuting Tu reported the iron leaching of SW in CWAO reaction.[9]

In recent years, the rapid growth of the coal chemical industry in China has posed problems because of the considerable quantities of cresol-containing wastewater. *m*-Cresol is more refractory than *o*-cresol and *p*-cresol and is one of the 11 phenolic compounds listed in the U.S. Environmental Protection Agency's priority contaminants.[13] Therefore, an efficient technique for treating cresol should be investigated. Compared to biological, electrochemical, ozonic, Fenton-like and photocatalytic treatments, CWAO is considered to be a more efficient method for treating high concentrations of organic pollutants.[14,15] In the past 20 years, a series of noble metal catalysts have been used in CWAO reaction and exhibited high activities.[16,17] However, these catalysts are considered to be too expensive for their utilisation in industrial CWAO application.[9] Compared to costly noble metal catalysts, the prepared SWs are low cost and could be used as catalysts in the CWAO reaction.

In this study, the surface of SW was modified by different kinds of acids. The element content, structure and valence state of the SW surface were measured. Furthermore, the effect of surface functional groups on catalytic activity in CWAO was discussed. On the basis of the intermediate products identified by GC-MS, HPLC-MS, IC and HRMS analyses, the oxidation pathways of *m*-cresol in CWAO were proposed.

a Dalian National Laboratory for Clean Energy, Dalian Institute of Chemical Physics, Chinese Academy of Sciences, Dalian 116023, PR China. E-mail: clsun@dicp.ac.cn; Fax: +86 411 84699965; Tel: +86 411 84379326
b University of Chinese Academy of Sciences, Beijing 100049, PR China

2. Materials and methods

2.1. Preparation and characterization of SWs

SWs were prepared by using municipal sewage sludge from a wastewater treatment plant (WWTP) in Dalian (China). Sewage sludge was dried to constant weight at 105 °C and carbonized at 600 °C for 4 h under a heating rate of 3 °C min^{-1} and a high purity nitrogen (99.999 wt%) flow of 500 mL min^{-1}. After the furnace had cooled to room temperature, SWs were obtained. In order to modify the surface of SWs, different acids were used to treat the SWs. In the acid treatment process, 50 mL of SWs were produced by immersing carbonized SWs with the same volume of HCl (20.5 wt%), H_2SO_4 (63.4 wt%) and HNO_3 (40.5 wt%) for 24 h, respectively. Then, HCl-SW, H_2SO_4-SW and HNO_3-SW were washed with deionized water until the pH of the washing water reached 6–7 and the recovered solids were dried at room temperature.

X-ray Fluorescence (XRF) was used to analyze the element content in the SW samples with Magix 601 equipment produced by PANalytical. Thermogravimetric analysis (TGA) (WRT-1D, China) was performed to measure the amount of carbon in SWs. The X-ray diffraction (XRD) spectra were obtained by using an X'Pert PRO instrument produced by PANalytical with Cu Kα (λ = 1.5406 Å) radiation at 40 kV and 40 mA in the 2θ scan range of 10–90°. The functional groups on the SWs were analyzed by Fourier Transform Infrared Spectroscopy (FTIR, Tensor 27, Germany). X-ray photoelectron spectroscopy (XPS) was performed to analyze the composition and chemical state of the surface elements of the SW catalysts. A Thermo ESCALAB250Xi instrument, with an Al K X-ray source (1486.6 eV) and a pass energy of 20 eV, was used at a pressure of 6.5×10^{-5} Pa. The binding energies were calibrated with respect to the signal for contamination carbon (binding energy = 284.6 eV). Temperature-programmed desorption (TPD) was used to measure the surface functional groups on the SW catalysts. The SW powder sample was treated at room temperature for 2 h under pure He (99.999%) flow. Then sample was heated up to 900 °C with a heating rate of 6 °C min^{-1} under pure He (99.999%) flow. The desorbed CO and CO_2 were detected with a mass spectrometer (Pfeiffer Vacuum, Ominstar GSD 301 O2).

2.2. Degradation experiments

The catalytic activity of the prepared SWs was assessed in a 500 mL batch reactor equipped with a magnetic stirrer and an electric heating jacket. The reactor was a CJF-0.5-type autoclave made of titanium alloy supplied by Dalian Tongda Autoclaves Plant. In a standard experiment, 200 mL of m-cresol (5000 mg L^{-1}) solution and 1 g of the catalyst were put into the autoclave. The size of the catalytic particles was less than 60 mesh. The reactor was closed and filled with a certain pressure of oxygen (6.6 bar), then the heating-up program was started. When the set temperature was attained, the stirring started at a speed of 600 rpm. This time was taken as the zero time and the liquid specimens were taken after 15 min, 30 min, 45 min, 60 min, 75 min and 90 min to measure the conversion of m-cresol and TOC removal. At the end of each experiment, the reactor was cooled down to room temperature and opened to recover the remaining SW catalyst. The catalyst was separated by filtration, whilst the remaining solution was stored for further analysis of the pH, m-cresol, TOC and metal ions leached from the catalyst.

The catalytic activity and stability of the SW catalysts in CWAO were tested in a fixed-bed reactor with upflow of m-cresol wastewater and air. The exact characteristics of the reactor and the catalyst bed are presented in Fig. S1 and S2.† The size of the catalytic particles was less than 2 mm. The gas and liquid flow rates were 40 mL min^{-1} and 0.17 mL min^{-1}, respectively. The operating temperature and reaction pressures ranged from 180 °C to 220 °C and 20 to 33 bar, respectively.

2.3. Analysis methods

All solutions used in this study were prepared in deionized water of 18.25 MΩ cm^{-1}. m-Cresol, nitric acid, sulfuric acid and hydrochloric acid were of analytical grade.

The concentration of m-cresol was analyzed via High-Performance Liquid Chromatography (HPLC). The HPLC system (Dalian Elite Analytic Instruments Co., Ltd) was equipped with an Elite C18 chromatographic column (4.6 mm × 250 mm, 5 μm) and a UV-detector set at 272 nm. The mobile phase was methanol : water = 80 : 20 (V/V) and the flow rate was fixed at 1.0 mL min^{-1}.

A total organic carbon (TOC) analyzer (TOC-V$_{CPH/CPN}$, Shimadzu, Japan) was employed to determine the residual amounts of organic substances in the effluent.

The pH of the m-cresol solution was measured using a REX PHS-3C pH meter (Rex Instrument Factory, Shanghai, China), and the meter was calibrated daily before use.

High-performance liquid chromatography-mass spectrometry (HPLC-MS) was used to investigate the intermediates in treated solutions by using an Agilent Q-TOF 6540 mass spectrometer.

Gas chromatography-mass spectrometry (GC-MS) was utilized to identify the intermediates in treated solutions. In order to detect the intermediate of low molecular weight acids from m-cresol degradation in CWAO, an esterification reaction was used to prepare the sample. The esterification method was given as follows. First of all, a liquid sample was concentrated through a rotary evaporator. Secondly, 2 mL of 10% (v/v) H_2SO_4 in alcohol was mixed with the residuals in a vial and placed in an oven at 60 °C for 8 h. While the mixture was cooled, it was neutralized with 1 mL of saturated Na_2CO_3. Then, 1 mL of hexane was added into the mixture to extract the fatty acids by stirring for 2 min. When the mixture settled, a pipette was used to remove the top hexane layer and transfer it into another vial. Finally, the dried hexane layer dried with Na_2SO_4 (anhydrous) to remove any residual water was filtered for GC-MS analyses. An Agilent model 7890A Gas Chromatograph (GC) equipped with a model 5975C mass selective detector and a capillary column (HP-5ms, 30 m ×

0.25 mm × 0.25 μm, Agilent J&W GC Columns) was used. The initial oven temperature of the gas chromatograph was kept at 50 °C for 5 min. The oven temperature increased at a rate of 15 °C min^{-1} to reach a final temperature of 250 °C, and this temperature was held for 10 min. The injection temperature was 250 °C. The detector temperature was 280 °C.

The low molecular weight acids were analyzed *via* ion chromatography (IC). The ICS-3000 system produced by DIONEX was equipped with an AS11-HC chromatographic column (4 mm × 250 mm). The temperatures of the column and cell heater were 30 °C and 35 °C, respectively. The mobile phase was 30 mol L^{-1} NaOH and the flow rate was fixed at 1.2 mL min^{-1}.

The chemical formula of the intermediates was determined by using a high-resolution mass spectrometer (HRMS) equipped with an electrospray ionization (ESI) source (Agilent Q-TOF 6540 mass spectrometer).

Nuclear magnetic resonance (NMR) was used to investigate the degradation of *m*-cresol. The ^{1}H NMR spectra were recorded on a Bruker DRX-400 spectrometer and the chemical shift values were referred to D$_2$O (δ(^{1}H), 4.79 ppm).

3. Results and discussion

3.1. Characterization of the catalysts

X-ray fluorescence (XRF) was used to measure the element content of SWs and the results are shown in Fig. 1. After the pyrolysis of sewage sludge, the content of carbon ranged from 74.3% to 13.8%. It indicated that most carbon element in the dried sludge transformed to gas and liquid (bio-oil) during the pyrolysis process. All samples had an extremely high content of SiO$_2$ and Al$_2$O$_3$, which was ascribed to the high content of inorganic compounds in the sludge. The contents of CaO were 9.7%, 1.0%, 1.9% and 0.5% in the SW, HNO$_3$-SW, H$_2$SO$_4$-SW and HCl-SW, respectively. Moreover the contents of Fe$_2$O$_3$ were 5.1%, 2.4%, 3.9% and 1.7% in the SW, HNO$_3$-SW, H$_2$SO$_4$-SW and HCl-SW, respectively. The

Table 1 BET surface area of SW catalysts

Catalysts	S_{BET} (N$_2$) (m^2 g^{-1})	Total pore volume (cm^3 g^{-1})	Pore diameter (nm)
SW	22	0.051	3.9
HNO$_3$-SW	53	0.049	3.8
H$_2$SO$_4$-SW	33	0.051	3.8
HCl-SW	81	0.083	3.9

results confirmed that CaO and Fe$_2$O$_3$ were partially removed by acid treatment.

The surface area of the SW catalysts is shown in Table 1. HCl-SW exhibited the largest surface area (81 m^2 g^{-1}) among the SW catalysts. The low surface area of the SW catalysts resulted from the high content of inorganics in the SW catalysts. The isothermal adsorption–desorption curves of the SW catalysts are shown in Fig. 2(a). The SW catalysts exhibited type IV adsorption isotherms. The pore size distribution of the SW catalysts is also shown in Fig. 2(b). HCl-SW had some micropores, which indicated that SW treated with HCl could form micropores.

The XRD patterns of the SW catalysts are shown in Fig. 3. The diffraction peaks at 2θ values of 20.9°, 26.6°, 36.5° and 64.0° were attributed to SiO$_2$. Moreover, the diffraction peaks at 2θ values of 29.4°, 39.4°, 43.2° and 57.5° were attributed to CaCO$_3$ and the peaks at 2θ values of about 37.0° and 46.0° were the characteristic peaks of Al$_2$O$_3$. In addition, the peaks at 2θ values of about 24.2°, 39.3° and 43.5° were attributed to Fe$_2$O$_3$. For H$_2$SO$_4$-SW, the diffraction peaks at 2θ values of 11.6°, 20.7° and 29.1° were attributed to CaSO$_4$. It indicated that after H$_2$SO$_4$ treatment, CaSO$_4$ was generated on the surface of the H$_2$SO$_4$-SW catalyst.

The FTIR spectra were used to investigate the surface groups of SWs, as shown in Fig. 4. All of the spectra exhibited a prominent broad peak at 3400–3500 cm^{-1}, which was attributed to the presence of water (hydroxyl groups). After the SWs were treated with HNO$_3$ and H$_2$SO$_4$, respectively, the peak at 1436 cm^{-1} disappeared while the peak at 1633 cm^{-1}

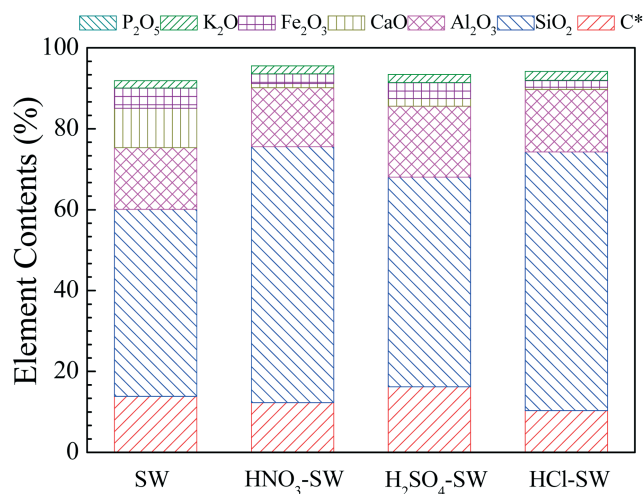**Fig. 1** XRF and TG analyses of elements in SWs treated with different acids: *detected by TG, other elements detected by XRF.
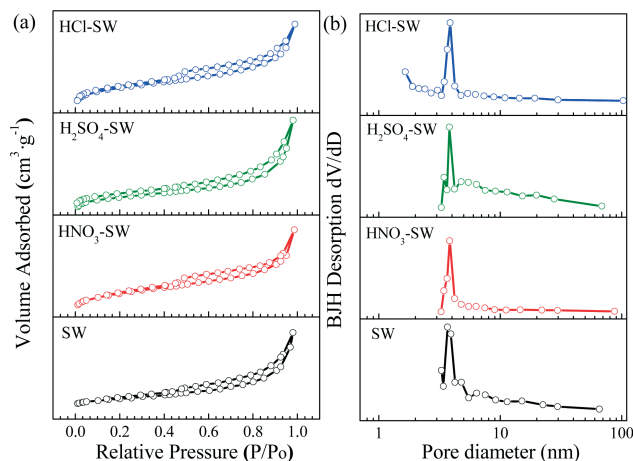

Fig. 2 Nitrogen adsorption/desorption isotherms (a) and pore distribution (b) of SW catalysts.
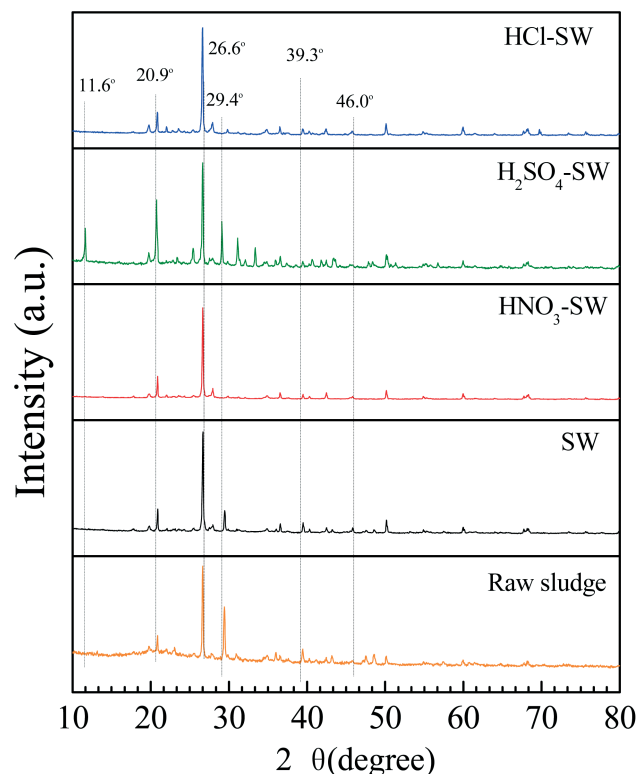
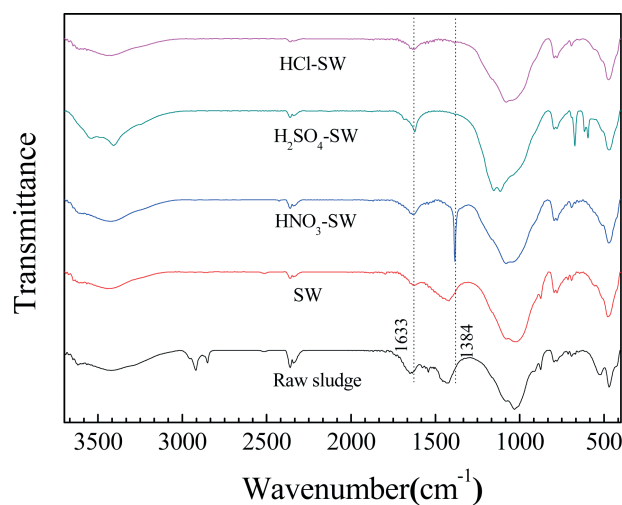**Fig. 3** XRD spectra of SWs treated with different acids.

Fig. 4 FTIR spectra of SWs treated with different acids.

related to C=O was strong and sharp, which indicated that the surface functional groups were replaced with C=O or carboxyl groups. Only HNO$_3$-SW exhibited a peak at 1384 cm^{-1}; this peak was broadly associated with nitrogen-containing compounds such as NO$_2$ groups.[1] The FTIR spectra demonstrated that the surface functional groups of SWs were modified by acid treatment.

The XPS C1s peaks of SW, HCl-SW, H$_2$SO$_4$-SW and HNO$_3$-SW are shown in Fig. 5. The deconvolution of the C1s spectra
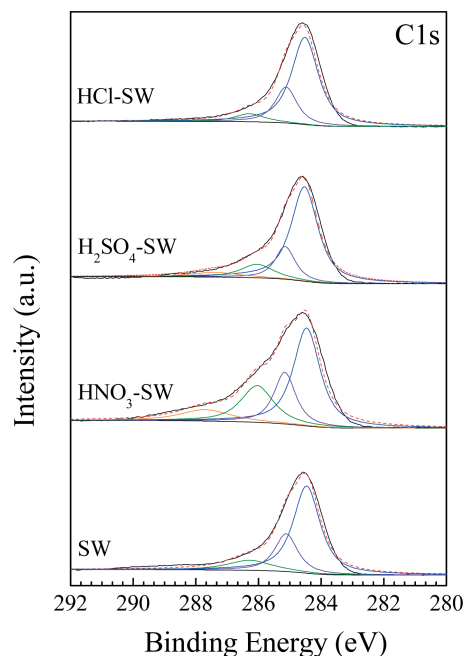

Fig. 5 Deconvolution of XPS C1s for SWs.

yielded the following four peaks: peak I (284.6 eV), carbon atoms in aliphatic/aromatic carbon (C–H, C–C and C=C); peak II (285.1–285.2 eV), carbon atoms in C–O; peak III (286.0–286.3 eV), carbon atoms in C=O; and peak IV (287.4–287.7 eV), carbon atoms in COOH, in a previous study.[18] Table 2 shows the list of their relative percentages on SWs. After SW was treated with HNO$_3$, C–C declined from 64.3% for SW to 47.8% for HNO$_3$-SW, and the content of C=O/COOH increased. It could be observed that the COOH group appeared after H$_2$SO$_4$ and HNO$_3$ treatment, respectively.

The XPS O1s peaks of SW, HCl-SW, H$_2$SO$_4$-SW and HNO$_3$-SW are shown in Fig. 6. The deconvolution of the O1s spectra yielded the following five peaks: peak I (533.1–533.5 eV), oxygen atoms in C–O; peak II (532.3–532.8 eV), oxygen atoms in SiO$_2$; peak III (531.7–532.3 eV), oxygen atoms in Si–O–Al; peak IV (531.2–531.7 eV), oxygen atoms in Al$_2$O$_3$; and peak V (530.4–531.0 eV), oxygen atoms in carbonate. The

Table 2 Deconvolution results of XPS C1s spectra of SWs

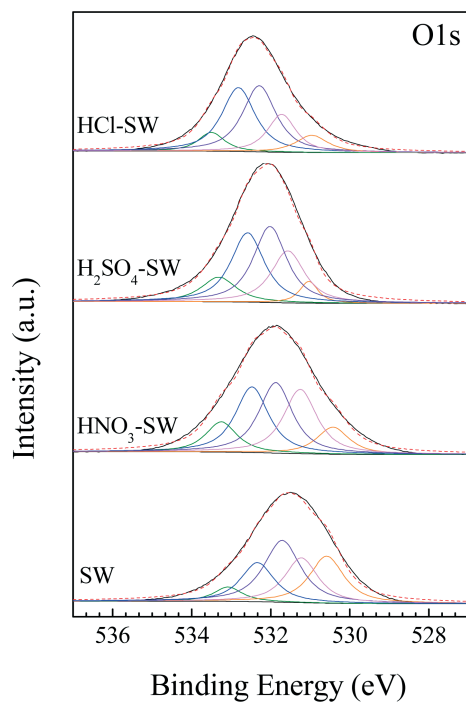| Sample	Peak	Position (eV)	FWHM (eV)	Area (%)
SW	C–C	284.6	1.02	64.3
	C–O	285.1	0.86	23.4
	C=O	286.3	1.69	12.3
HNO$_3$-SW	C–C	284.6	1.02	47.8
	C–O	285.2	0.82	20.3
	C=O	286.0	1.23	21.6
	COOH	287.7	1.90	10.3
H$_2$SO$_4$-SW	C–C	284.6	1.02	65.7
	C–O	285.2	0.75	17.4
	C=O	286.0	1.23	10.8
	COOH	287.4	1.90	6.1
HCl-SW	C–C	284.6	1.02	69.8
	C–O	285.1	0.82	23.1
	C=O	286.3	1.13	7.1

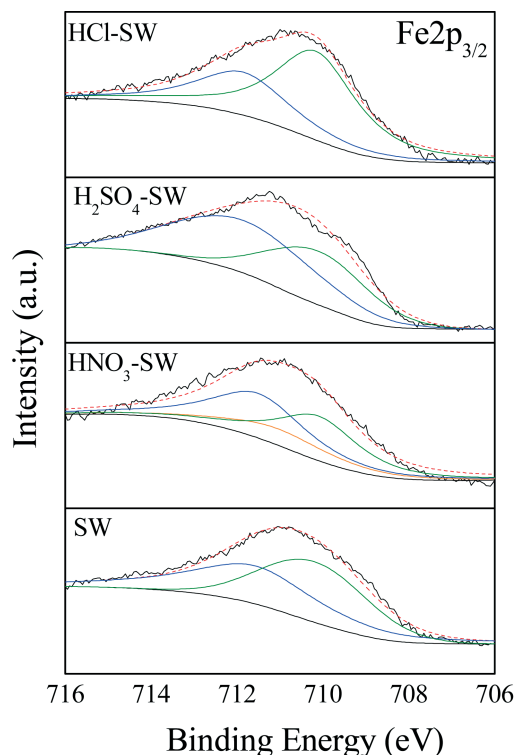**Fig. 6** Deconvolution of XPS O1s for SWs.

Fig. 7 Deconvolution of XPS Fe2p$_{3/2}$ for SWs.

Table 3 Deconvolution results of XPS O1s spectra of SWs

Sample	Peak	Position (eV)	FWHM (eV)	Area (%)
SW	C–O	533.1	0.85	5.7
	SiO_2	532.3	1.00	18.4
	Si–O–Al	531.7	1.10	32.0
	Al_2O_3	531.2	1.00	21.0
	Carbonate	530.6	1.03	22.9
HNO_3-SW	C–O	533.3	0.94	11.1
	SiO_2	532.3	1.00	25.7
	Si–O–Al	531.7	1.10	27.7
	Al_2O_3	531.3	1.00	25.2
	Carbonate	530.4	0.97	10.3
H_2SO_4-SW	C–O	533.3	1.04	10.9
	SiO_2	532.6	1.00	29.4
	Si–O–Al	532.0	1.00	32.4
	Al_2O_3	531.6	1.00	22.1
	Carbonate	531.0	0.56	5.2
HCl-SW	C–O	533.5	0.77	7.6
	SiO_2	532.8	1.00	33.0
	Si–O–Al	532.3	1.00	34.1
	Al_2O_3	531.7	0.85	16.7
	Carbonate	531.0	0.97	8.6

deconvolution results of the XPS O1s spectra of SWs are shown in Table 3. It indicated that the content of SiO_2 increased after acid treatment and the content of C–O also increased by oxidizing acid treatment.

The XPS Fe2p$_{3/2}$ peaks of SW, HCl-SW, H_2SO_4-SW and HNO_3-SW are presented in Fig. 7. The peak at 711.5–711.9 eV was assigned to Fe^{2+} and the peak at 710.1–710.2 eV was assigned to Fe^{3+}.[19] The deconvolution results of the XPS Fe2p$_{3/2}$ spectra of SWs are shown in Table 4. It could be

observed that Fe_3O_4 (711.0 eV) appeared after HNO_3 treatment. There is some controversy in the literature with respect to the assignment of TPD peaks to specific surface groups, because the peak temperatures are known to be affected by the porous texture of the material, the heating rate, and the geometry of the experimental system used.[20] However, some general trends have been established for the oxygen-containing groups. The CO_2 peak results from carboxylic acids at low temperature ($t < 430$ °C) and from lactones at higher temperatures (430–630 °C). Carboxylic anhydrides produce both CO and CO_2 peaks, while phenols and carbonyls produce a CO peak at temperatures above 630 °C. The TPD spectra obtained from the carbon materials display overlapping data from different contributions, and should thus be deconvoluted to determine each individual contribution from specific oxygen surface groups.[21] The CO and CO_2 TPD spectra obtained from SWs are shown in Fig. 8. It

Table 4 Deconvolution results of XPS Fe2p$_{3/2}$ spectra of SWs

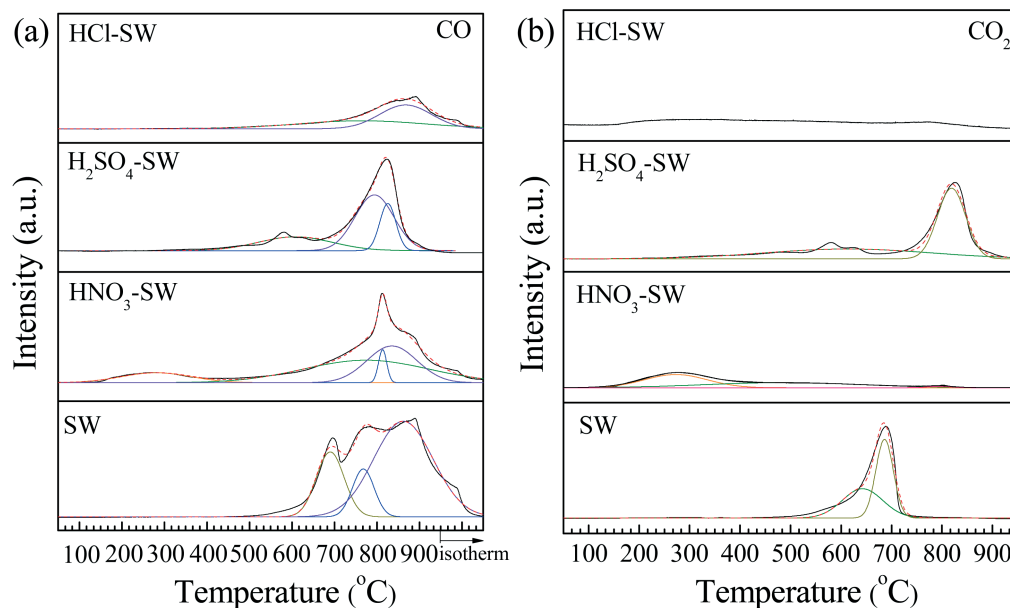| Sample	Peak	Position (eV)	FWHM (eV)	Area (%)
SW	Fe(II)	710.2	2.92	48.4
	Fe(III)	711.6	3.50	51.6
HNO_3-SW	Fe(II)	710.1	2.30	37.9
	Fe_3O_4	711.0	3.13	19.0
	Fe(III)	711.5	2.62	43.1
H_2SO_4-SW	Fe(II)	710.1	2.74	41.4
	Fe(III)	711.9	3.97	58.6
HCl-SW	Fe(II)	710.2	2.29	64.9
	Fe(III)	711.9	2.57	35.1

Fig. 8 TPD spectra and deconvolution of SWs: CO (a) and CO_2 (b).

Table 5 TPD deconvolution of CO and CO_2 spectra for SWs

Sample	CO-evolving groups (%)					CO_2-evolving groups (%)			
	Carboxylic	Anhydride	Ether	Carbonyl	Phenol	Carboxylic	Anhydride	Lactone	Carbonate
SW	—	—	12.2	66.6	21.2	—	—	46.1	53.9
HNO$_3$-SW	12.3	50.0	4.8	32.9	—	—	48.3	2.0	—
H$_2$SO$_4$-SW	—	25.9	55.0	19.1	—	—	44.4	—	55.6
HCl-SW	—	45.4	—	54.6	—	—	—	—	—

indicated that CO evolution was more significant than CO_2 evolution. The deconvolution of the CO_2 spectra showed four contributions attributed to carboxylic acid groups (peak at 240–280 °C), anhydrides (peak at 410–490 °C), lactones (peak at 610–650 °C) and carbonates (peak at 680–750 °C). The other peaks observed for the CO TPD spectra of SWs were attributed to carboxylic acid groups (peak at 240–280 °C), anhydrides (peak at 400–700 °C), ethers (peak at 750–800 °C), carbonyls (peak at 820–870 °C) and phenols (peak at 690 °C). The total amount of CO and CO_2 evolved, as obtained by integration of the areas under the curves, is indicated in each case. The assessment of surface oxygen groups was performed according to literature criteria,[21–23] as shown in Table 5. The results showed that the SW surface functional groups were modified by acid treatment. For SW, the total content of basic groups such as ether, carbonyl, lactone and phenol was the highest among SWs and the basic groups decreased after acid treatment. HNO$_3$-SW showed the highest content of carboxylic groups, both in terms of CO and CO_2 releasing groups. The carboxylic groups were assigned as strongly acidic sites and might be beneficial to CWAO reaction. After H$_2$SO$_4$ treatment, the surface of H$_2$SO$_4$-SW was modified by sulfoacid groups and the desorption temperature of the CO_2 TPD was higher than SW. Due to the weak oxidation of HCl, the HCl-SW surface functional groups decreased

significantly by the acid–base neutralization reaction and few carboxylic groups were formed.

3.2. Oxidation of m-cresol in the batch reactor

The m-cresol conversion and TOC removal at different times of CWAO reaction are shown in Fig. 9. The results showed that HNO$_3$-SW yielded the highest levels of m-cresol conversion (99.0%) and TOC removal (67.9%) at 160 °C and 6.6 bar of oxygen pressure. The pH values of the effluents were 7.07, 2.98, 2.18 and 2.70 for SW, HNO$_3$-SW, H$_2$SO$_4$-SW and HCl-SW, respectively. The final values of gas pressure were 3.0 bar, 2.7 bar, 2.8 bar and 2.9 bar for SW, HNO$_3$-SW, H$_2$SO$_4$-SW and HCl-SW, respectively. After the oxidizing acid treatment, the catalytic activities of HNO$_3$-SW and H$_2$SO$_4$-SW greatly increased, respectively, and were much higher than those of SW and HCl-SW. From the XRF data, all of the SWs exhibited quantities of Fe$_2$O$_3$ (>1.5 wt%) and hence could be considered as active sites. However, the content of Fe$_2$O$_3$ in SW was the highest (5.1 wt%), while the catalytic activity of SW was the lowest. It indicated that the content of iron in SWs might not be the only factor for the high catalytic activity in CWAO. After CWAO reaction, the amounts of iron leached were 1.2 mg L^{-1}, 10.8 mg L^{-1}, 11.7 mg L^{-1} and 0.8 mg L^{-1} for SW, HNO$_3$-SW, H$_2$SO$_4$-SW and HCl-SW, respectively. The iron
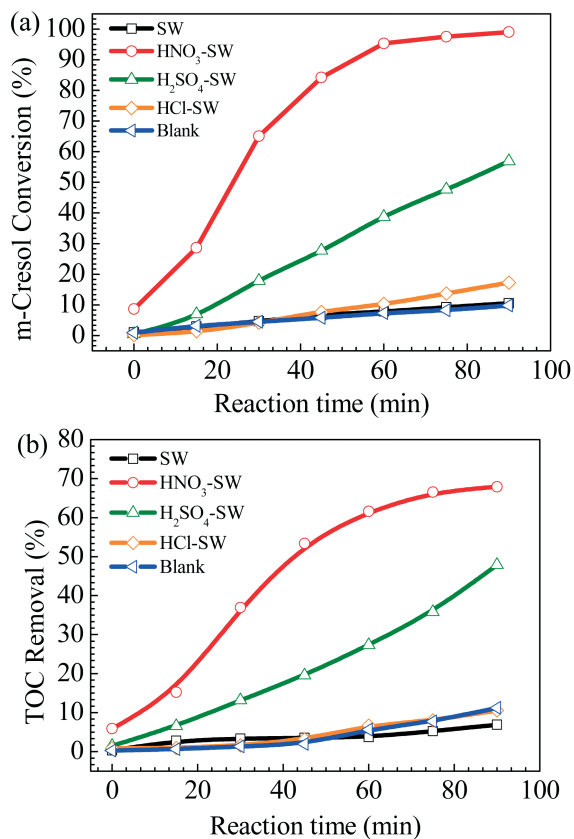
Fig. 9 Effect of SW catalysts on *m*-cresol conversion (a) and TOC removal (b) in batch CWAO reaction. Reaction conditions: P_{O_2} = 6.6 bar, T = 160 °C, $C_{m\text{-cresol}}$ = 5000 mg L^{-1}, initial pH = 7, $W_{catalyst}$ = 5 g L^{-1}.
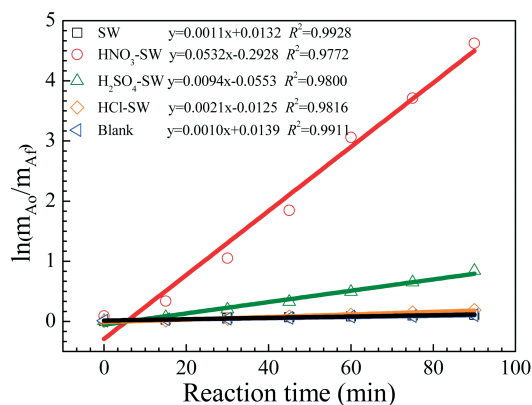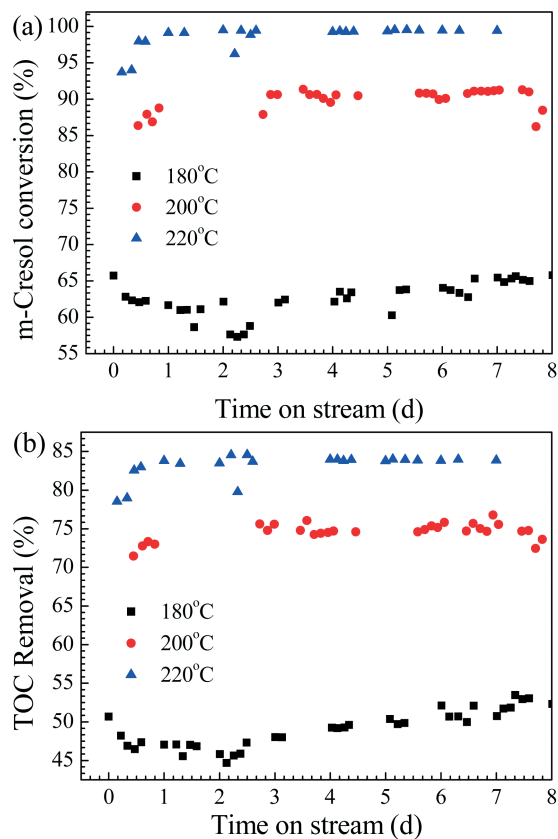

Fig. 11 Effect of temperature on *m*-cresol conversion (a) and TOC removal (b) with HNO$_3$-SW in continuous CWAO reaction. Reaction conditions: $C_{m\text{-cresol}}$ = 5000 mg L^{-1}, LHSV = 1 h^{-1}, initial pH = 7.

of *m*-cresol, m_{Af}: the concentration of *m*-cresol in the reaction process). It was found that the degradation of *m*-cresol in CWAO obeyed the first-order kinetic model. The reaction rate constant k of *m*-cresol in CWAO with SWs was obtained according to the slope of the fitted line. The first-order rate constant k values were 0.0011, 0.0532, 0.0094, and 0.0021 for SW, HNO$_3$-SW, H$_2$SO$_4$-SW and HCl-SW, respectively. HNO$_3$-SW

Fig. 10 Kinetic plots for *m*-cresol in CWAO reaction.

leaching of H$_2$SO$_4$-SW was the highest (11.7 mg L^{-1}); however, HNO$_3$-SW exhibited the highest catalytic activity. It indicated that a homogeneous reaction was not the only factor for the high catalytic activity of HNO$_3$-SW. Other factors such as the surface functional groups of SWs were also investigated.

According to the data in Fig. 10, linear fitting was done between ln(m_{Ao}/m_{Af}) and time (m_{Ao}: the initial concentration
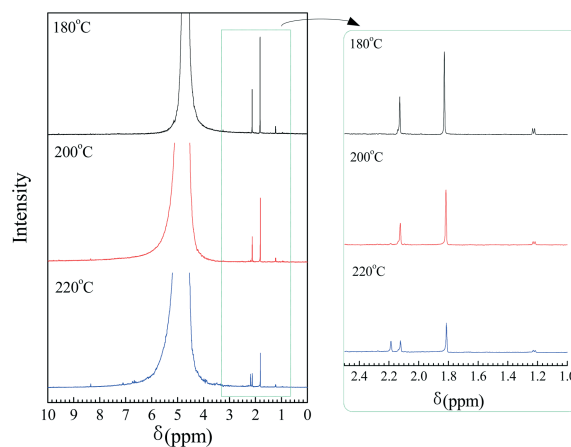

Fig. 12 ^{1}H NMR spectra of *m*-cresol in CWAO reaction at different temperatures.
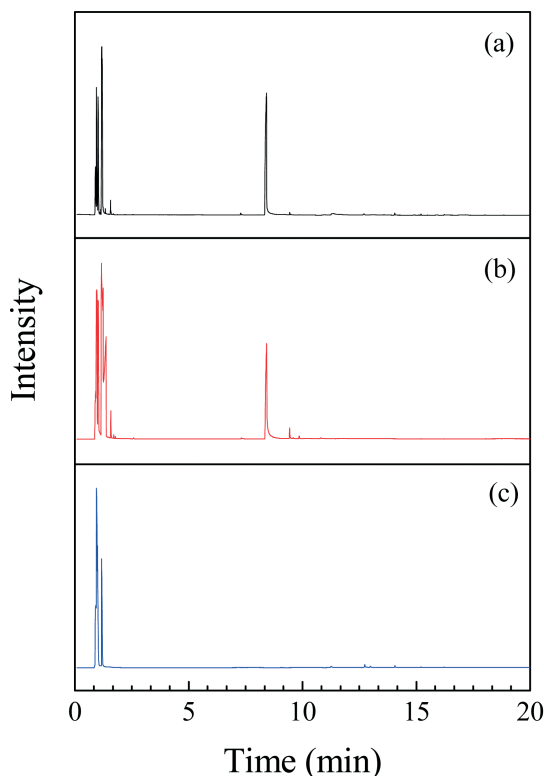
Fig. 13 GC-MS spectra of *m*-cresol in CWAO reaction at different times: 60 min (a), 120 min (b) and 180 min (c).

Fig. 14 Possible degradation pathway of *m*-cresol in CWAO by the HNO₃-SW catalyst. **1**–**10** carboxylic acids were detected by GC-MS and HRMS in this work, **A**–**F** compounds are degradation intermediates.

exhibited the highest reaction rate constant (k = 0.0532) among the SWs. The FTIR data (Fig. 3), XPS C1s spectra (Fig. 5) and TPD (Fig. 8) spectra provided direct evidence for the existence of carboxylic acid groups on HNO₃-SW. The high content of carboxylic groups on HNO₃-SW was therefore the primary determinant of the high catalytic activity.

3.3. Oxidation of *m*-cresol in the continuous reactor

Short-term experiments conducted at different temperatures (180–220 °C) revealed that temperature had a great effect on *m*-cresol conversion by the HNO₃-SW catalyst in continuous CWAO reaction, and the results are shown in Fig. 11. The TOC removal was about 50% at 180 °C and it reached about 75% and 85% at 200 °C and 220 °C, respectively. It indicated that high temperature could improve the degradation of *m*-cresol in a continuous CWAO reaction.

The degradation of *m*-cresol was investigated in NMR. It is shown in Fig. 12 that the ¹H NMR (D₂O, 400 MHz) peaks at δ 2.5–1.0 were attributed to alkyl H. With the temperature increasing, the peaks of *m*-cresol in ¹H NMR spectra were weak. It indicated that high temperature could improve the degradation of *m*-cresol in CWAO reaction.

3.4. *m*-Cresol oxidation mechanism in CWAO reaction

In order to investigate the degradation pathway of *m*-cresol in the process of CWAO by the HNO₃-SW catalyst, GC-MS, IC, HPLC-MS and HRMS were applied to identify the organic course pro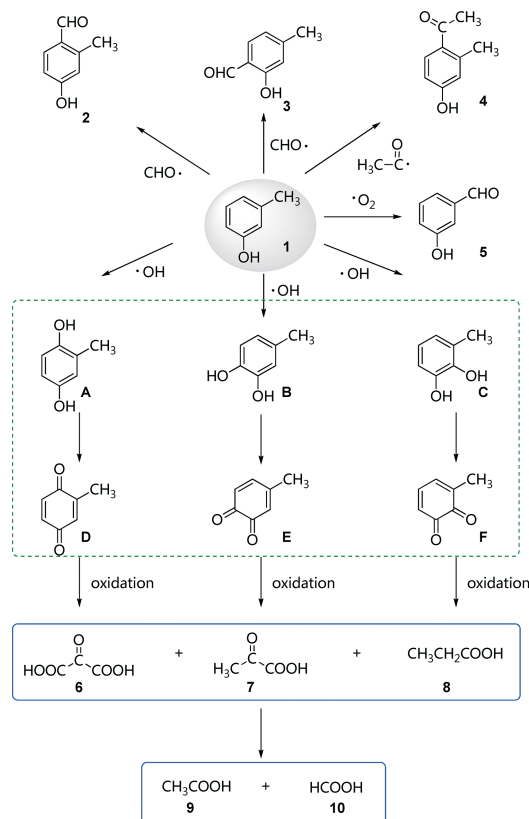ducts, and the results are shown in Fig. 13, S3–S5 and Table S1.† It indicated that the degradation of *m*-cresol in CWAO reaction was rapid and the intermediates were rapidly oxidized to low molecular weight acids (less than 3 carbon atoms). In the CWAO experiment of *m*-cresol, 9 kinds of intermediates were identified (Fig. 14). It was proposed that *m*-cresol might be degraded in three pathways, similar to phenol in previous reports.[24,25] In the first step, ˙OH attacked the *ortho* and *para* positions of *m*-cresol and formed 2-methylbenzene-1,4-diol (**A**), 4-methylbenzene-1,2-diol (**B**) and 3-methylbenzene-1,2-diol (**C**), and then **A**, **B** and **C** were quickly oxidized to quinones **D**, **E** and **F**, respectively. Secondly, quinones **D**, **E** and **F** were oxidized to low molecular weight acids such as 2-oxomalonic acid (**6**), 2-oxopropanoic acid (**7**), propionic acid (**8**), acetic acid (**9**) and formic acid (**10**). Subsequently, other free radicals, ˙CHO, CH₃CO˙ and O₂˙, attacked *m*-cresol and formed 4-hydroxy-2-methylbenzaldehyde (**2**), 2-hydroxy-4-methylbenzaldehyde (**3**), 1-(4-hydroxy-2-methylphenyl)ethanone (**4**) and 3-hydroxybenzaldehyde (**5**).

Conclusions

In this study, the catalytic activity of surface-modified sewage sludge-derived carbonaceous materials (SW) was investigated in catalytic wet air oxidation (CWAO) reaction. SW treated

with oxidizing acids such as H_2SO_4 and HNO_3 showed high catalytic activity in the catalytic wet air oxidation of *m*-cresol. The high catalytic activity of SW was ascribed to the high content of iron and surface functional groups. The degradation of *m*-cresol in CWAO could be described by the first-order kinetic model. The degradation of *m*-cresol by the CWAO process mainly generated four cyclic organic intermediates and several short-chain carboxylic acids. The HNO_3-SW catalyst showed good stability in continuous CWAO reaction.

References

1 R. R. N. Marques, F. Stüber, K. M. Smith, A. Fabregat, C. Bengoa, J. Font, A. Fortuny, S. Pullket, G. D. Fowler and N. J. D. Graham, *Appl. Catal., B*, 2011, **101**, 306–316.

2 L. Yu, W. Jiang, Y. Yu and C. Sun, *Environ. Technol.*, 2014, **35**, 3092–3104.

3 K. M. Smith, G. D. Fowler, S. Pullket and N. J. D. Graham, *Sep. Purif. Technol.*, 2012, **98**, 240–248.

4 M. Agarwal, J. Tardio and S. V. Mohan, *Bioresour. Technol.*, 2015, **178**, 70–75.

5 Q. L. Xie, P. Peng, S. Y. Liu, M. Min, Y. L. Cheng, Y. Q. Wan, Y. Li, X. Y. Lin, Y. H. Liu, P. Chen and R. Ruan, *Bioresour. Technol.*, 2014, **172**, 162–168.

6 L. L. Yu and Q. Zhong, *J. Hazard. Mater.*, 2006, **137**, 359–366.

7 K. M. Smith, G. D. Fowler, S. Pullket and N. J. D. Graham, *Water Res.*, 2009, **43**, 2569–2594.

8 F. Stüber, K. M. Smith, M. Baricot Mendoza, R. R. N. Marques, A. Fabregat, C. Bengoa, J. Font, A. Fortuny, S. Pullket, G. D. Fowler and N. J. D. Graham, *Appl. Catal., B*, 2011, **110**, 81–89.

9 Y. T. Tu, Y. Xiong, S. H. Tian, L. J. Kong and C. Descorme, *J. Hazard. Mater.*, 2014, **276**, 88–96.

10 G. Wen, Z. H. Pan, J. Ma, Z. Q. Liu, L. Zhao and J. J. Li, *J. Hazard. Mater.*, 2012, **239**, 381–388.

11 Y. Tu, S. Tian, L. Kong and Y. Xiong, *Chem. Eng. J.*, 2012, **185**, 44–51.

12 L. Gu, N. Zhu, H. Guo, S. Huang, Z. Lou and H. Yuan, *J. Hazard. Mater.*, 2013, **246**, 145–153.

13 P. J. Liu, S. B. He, H. Z. Wei, J. H. Wang and C. L. Sun, *Ind. Eng. Chem. Res.*, 2015, **54**, 130–136.

14 H. Z. Wei, X. M. Yan, S. B. He and C. L. Sun, *Catal. Today*, 2013, **201**, 49–56.

15 H. Z. Wei, X. M. Yan, X. R. Li, S. B. He and C. L. Sun, *J. Hazard. Mater.*, 2013, **244**, 478–488.

16 N. Li, C. Descorme and M. Besson, *Appl. Catal., B*, 2008, **80**, 237–247.

17 J. Gaalova, J. Barbier-Jr and S. Rossignol, *J. Hazard. Mater.*, 2010, **181**, 633–639.

18 Q. L. Fang, B. L. Chen, Y. J. Lin and Y. T. Guan, *Environ. Sci. Technol.*, 2014, **48**, 279–288.

19 P. Boron, L. Chmielarz, J. Gurgul, K. Latka, B. Gil, B. Marszalek and S. Dzwigaj, *Microporous Mesoporous Mater.*, 2015, **203**, 73–85.

20 J. L. Figueiredo, M. F. R. Pereira, M. M. A. Freitas and J. J. M. Orfao, *Ind. Eng. Chem. Res.*, 2007, **46**, 4110–4115.

21 H. F. Gorgulho, J. P. Mesquita, F. Goncalves, M. F. R. Pereira and J. L. Figueiredo, *Carbon*, 2008, **46**, 1544–1555.

22 J. L. Figueiredo, M. F. R. Pereira, M. M. A. Freitas and J. J. M. Órfão, *Carbon*, 1999, **37**, 1379–1389.

23 J. H. Zhou, Z. J. Sui, J. Zhu, P. Li, D. Chen, Y. C. Dai and W. K. Yuan, *Carbon*, 2007, **45**, 785–796.

24 Y. Chu, D. Zhang, L. Liu, Y. Qian and L. Li, *J. Hazard. Mater.*, 2013, **252**, 306–312.

25 P. Liu, S. He, H. Wei, J. Wang and C. Sun, *Ind. Eng. Chem. Res.*, 2015, **54**, 130–136.